Group 4 Metal Atom Reactions with CF_3Cl, $CFCl_3$, CF_3Br, and CF_3I: A Matrix Infrared Spectroscopic and DFT Investigation of Competitive α-Halogen Transfer to Form Triplet $XC{\div}MX_3$ Complexes

Jonathan T. Lyon and Lester Andrews*

Department of Chemistry, University of Virginia, P.O. Box 400319, Charlottesville, Virginia 22904-4319

Received March 5, 2007

Laser-ablated group 4 transition metal atoms react with $CX^1X^2_3$ (X = F, Cl, Br, or I) to form triplet state $X^1C{\div}MX^2_3$ and $X^2C{\div}MX^1X^2_2$ complexes, which are identified by their infrared spectra, carbon-13 isotopic shifts, and comparison to density functional vibrational frequency calculations. The higher energy product with more heavier halogen migration converts to the lower energy product with more α-F transfer on UV irradiation. Two features are of particular interest in these product complexes: The first is the presence of a very strong C−X bond, and the second is that the two unpaired electrons on carbon are shared with the transition metal center, forming an electron-deficient triple bond. Comparisons are made to the analogous reaction products with CF_4, CCl_4, and CF_2Cl_2.

Introduction

Activation of C−H bonds is an integral step in many industrial processes and has been studied on many levels. Recently, activation of carbon−halogen bonds has emerged as an attractive field of research.[1−4] This interests stems, in part, from the role activation plays in the remediation of chlorofluorocarbons, which are hazardous to the earth's atmosphere and are efficient greenhouse gases.[5−7] However, C−F bonds are the strongest carbon single bond and activation is not always a trivial task.[8]

Recent metal atom investigations with CH_3X (X = F, Cl, and Br) have shown that group 4 metals can activate the C−X bonds and promote α-H transfer.[9] In these studies, the main reaction products are the simple $CH_2{=}MHX$ methylidenes, which show considerable agostic distortion. Metal atom reactions with CH_2X_2 form analogous $CH_2{=}MX_2$ complexes without agostic interaction.[10−12] Titanium reacted with CHF_3 to form a similar $CHF{=}TiF_2$ methylidene complex, but Zr and Hf reactions produced triplet $HC{\div}MF_3$ complexes.[11] Here the two unpaired electrons on carbon are shared with the electron-deficient metal center, forming a partially occupied triple bond. Group 4 reactions with $CHCl_3$ yielded the analogous $HC{\div}MCl_3$ complexes.[12] The triplet $FC{\div}MF_3$ and $ClC{\div}MCl_3$ species showed even more donation of the unpaired electron density to the metal center and possessed some of the strongest single carbon−halogen bonds known.[13,14] Interestingly, reactions with CF_2Cl_2 yielded a mixture of analogous $FC{\div}MFCl_2$ and $ClC{\div}MF_2Cl$ complexes.[14]

We now react CF_3Cl, $CFCl_3$, CF_3Br, and CF_3I with the group 4 transition metals with two questions in mind. First, we want to compare the reaction products that form along the series CF_4, CF_3Cl, CF_2Cl_2, $CFCl_3$, and CCl_4. This will provide a detailed investigation of how chlorine substitution alters the reaction pathway and affects the stability of the reaction product. Second, we would like to investigate which reaction products form ($ClC{\div}MX_3$, $BrC{\div}MF_3$, or $FC{\div}MX_3$) in the reactions with CF_3Cl, CF_3Br, and $CFCl_3$. Third, we wish to determine how bromine and iodine substitution alter the pathway in the reactions of the group 4 metal atoms with CF_3Cl, CF_3Br, and CF_3I.

Experimental and Theoretical Methods

Our experimental setup has been described elsewhere.[9,15] In brief, laser-ablated metal atoms (Nd:YAG laser; 1064 nm, 10 Hz repetition rate, 10 ns pulse width) were co-deposited with a dilute mixture (0.1−0.5%) of halocarbon reagent gas in argon onto a CsI window cooled to 8 K for the duration of 1 h. Infrared spectra were then collected of the matrix-isolated reaction products at 0.5 cm^{-1} resolution by a Nicolet Magna 550 spectrometer with a MCT type B detector. Matrixes were subjected to annealing to various temperatures (typically around 30 K) and irradiation by a medium-pressure mercury arc lamp (Philips, 175 W, $\lambda > 220$ nm) filtered to pass desired wavelengths. Additional IR spectra were collected after each procedure.

Computations were carried out using the Gaussian 98 program,[16] and the B3LYP hybrid density functional was employed for the calculations of possible reaction product energies and vibrational frequencies.[17] This functional has been shown to provide accurate results in similar studies.[9−14] The carbon and halogen atoms were

* Corresponding author. E-mail: lsa@virginia.edu.

(1) (a) Kiplinger, J. L.; Richmond, T. G.; Osterberg, C. E. *Chem. Rev.* **1994**, *94*, 373. (b) Burdeniuc, J.; Jedlicka, B.; Crabtree, R. H. *Chem. Ber.* **1997**, *130*, 145.
(2) Mazurek, U.; Schwarz, H. *Chem. Commun.* **2003**, 1321.
(3) Edelbach, B. L.; Rahman, A. K. F.; Lachicotte, R. J.; Jones, W. D. *Organometallics* **1999**, *18*, 3170.
(4) Reinhold, M.; McGrady, J. E.; Perutz, R. N. *J. Am. Chem. Soc.* **2004**, *126*, 5268.
(5) Molina, M. J.; Rowland, F. S. *Nature* **1974**, *249*, 810.
(6) Victor, D. G.; MacDonald, G. J. *Clim. Change* **1999**, *42*, 633.
(7) Timms, P. L. *J. Chem. Soc., Dalton Trans.* **1999**, 815.
(8) Strauss, S. H. *Chem. Rev.* **1993**, *93*, 927.
(9) Andrews, L.; Cho, H.-G. *Organometallics* **2006**, *25*, 4040, and references therein.
(10) Lyon, J. T.; Andrews, L. *Organometallics* **2006**, *25*, 1341.
(11) Lyon, J. T.; Andrews, L. *Inorg. Chem.* **2007**, *46*, 4799.
(12) Lyon, J. T.; Andrews, L. *Organometallics* **2007**, *26*, 332.
(13) Lyon, J. T.; Andrews, L. *Inorg. Chem.* **2006**, *45*, 9858.
(14) Lyon, J. T.; Andrews, L. *Organometallics* **2007**, *26*, 2519 (group 4 + CX_4 and CF_2Cl_2).
(15) Andrews, L. *Chem. Soc. Rev.* **2004**, *33*, 123.

10.1021/om0702025 CCC: $37.00
Publication on Web 07/21/2007

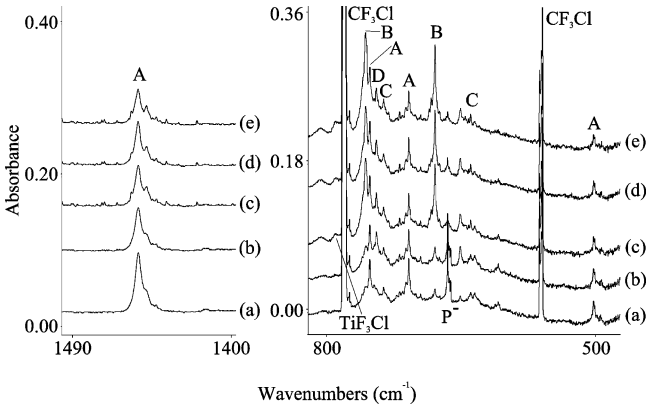

Figure 1. Infrared spectra in the 1490−1400 and 820−470 cm^{-1} regions taken after (a) laser-ablated titanium atoms were reacted with 0.5% CF_3Cl/Ar during condensation at 8 K for 1 h, and the resulting matrix was subjected to (b) irradiation with light $\lambda > 290$ nm, (c) irradiation with $\lambda > 220$ nm, (d) annealing to 30 K, and (e) irradiation with $\lambda > 220$ nm. Product absorptions labeled A belong to the FC÷TiF_2Cl complex, B peaks are assigned to the ClC÷TiF_3 species, and the identity of C and D peaks is not resolved at this time. The P^- absorption was observed and identified in ref 20b.

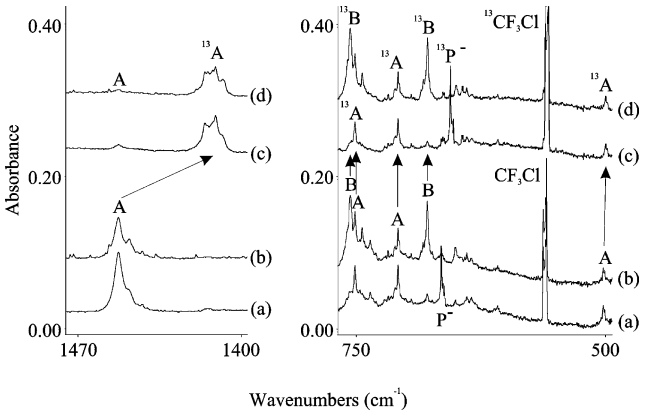

Figure 2. IR spectra in the 1470−1400 and 770−490 cm^{-1} regions of the spectra taken after (a) laser-ablated titanium atoms were reacted with 0.5% CF_3Cl/Ar, and (b) the matrix sample was irradiated with $\lambda > 220$ nm, and after (c) titanium atoms were reacted with 0.5% $^{13}CF_3Cl$/Ar, and (d) the matrix sample was irradiated with $\lambda > 220$ nm. Arrows are shown for only A and B product peaks.

given 6-311+G(2d) basis sets,[18] whereas the electronic densities of the transition metal centers were represented by the SDD pseudopotential.[19] All energy values reported include zero-point vibrational corrections.

Results and Discussion

The reaction products of group 4 transition metals with CF_3Cl, $CFCl_3$, CF_3Br, and CF_3I will be characterized by matrix infrared spectra and density functional theory calculations. These experiments reveal absorptions due to precursor fragment reactive species that have been reported previously.[20]

Ti + CF_3Cl. Reactions between laser-ablated titanium atoms and CF_3Cl (Freon-13) produced five groups of product absorptions. The main group A absorptions observed at 502.0, 708.4, 751.8, and 1452.6 cm^{-1} decreased in intensity on all irradiations and increased slightly on annealing (Figure 1). The highest observed absorption at 1452.6 cm^{-1} showed a relatively large, 41.5 cm^{-1} ^{13}C isotopic shift (Figure 2) and can be assigned to a C−F stretching mode. Note that this frequency is considerably higher than that of the antisymmetric C−F stretching mode of the CF_3Cl precursor absorption at 1205 cm^{-1}. Such a high observed mode in similar experiments with CF_4 became the diagnostic frequency of the C−F bond in FC÷TiF_3.[13,14] Hence, it seems likely that these group A absorptions belong to the FC÷TiF_2Cl complex. Indeed, the next two bands observed at 751.8 and 708.4 cm^{-1} show no carbon-13 shifts and are in the region where Ti−F stretching modes are expected.[21] The fourth product peak at 502.0 cm^{-1} shows only a slight shift upon carbon-13 isotopic substitution and fits our B3LYP calculation for the vibrational mode with a single titanium atom stretching against the (CF) subunit in the triplet FC÷TiF_2Cl complex (Table 1) considering the approximations involved.[13,14,22,23]

Table 1. Observed and Calculated Fundamental Frequencies of FC÷TiF_2Cl[a]

	FC÷TiF_2Cl		F^{13}C÷TiF_2Cl	
approximate mode	obsd[b]	calcd (int)	obsd[b]	calcd (int)
FCTi bend		66.7 (0)		66.6 (0)
FCTi bend		71.6 (0)		71.1 (0)
ClTiF bend		144.1 (2)		144.1 (2)
FTiF bend		158.8 (3)		158.0 (3)
TiF_2Cl umbrella		180.9 (7)		180.5 (7)
FCTi def		207.0 (3)		202.0 (3)
FCTi def		228.2 (3)		221.7 (3)
Ti−Cl stretch	*c*	431.7 (44)	*c*	430.7 (43)
(FC)÷Ti stretch	502.0	502.0 (132)	499.6	500.6 (133)
Ti−F stretch	708.4	724.6 (211)	708.4	724.6 (211)
Ti−F stretch	751.8	765.8 (206)	751.8	765.8 (206)
C−F stretch	1452.6	1470.5 (364)	1411.1	1429.7 (348)

[a] B3LYP//6-311+G(2d)/SDD level of theory. All frequencies are unscaled and in cm^{-1}, and computed infrared intensities are in km/mol. [b] Argon matrix. [c] Absorption below our spectral limit.

Group B absorptions at 679.2 and 756.6 cm^{-1} increased slightly when exposed to Pyrex-filtered UV light ($\lambda > 290$ nm) and increased substantially on full-arc photolysis ($\lambda > 220$ nm) at the expense of the A bands. Both absorptions showed practically no ^{13}C isotopic shifts and can be assigned to Ti−F stretching modes. Following previous reaction pathway arguments,[11−14] two possible products need to be considered for the group B absorptions. The first is the singlet CFCl═TiF_2 methylidene,

(16) Frisch, M. J.; Trucks, G. W.; Schlegel, H. B.; Scuseria, G. E.; Robb, M. A.; Cheeseman, J. R.; Zakrzewski, V. G.; Montgomery, J. A., Jr.; Stratmann, R. E.; Burant, J. C.; Dapprich, S.; Millam, J. M.; Daniels, A. D.; Kudin, K. N.; Strain, M. C.; Farkas, O.; Tomasi, J.; Barone, V.; Cossi, M.; Cammi, R.; Mennucci, B.; Pomelli C.; Adamo, C.; Clifford, S.; Ochterski, J.; Petersson, G. A.; Ayala, P. Y.; Cui, Q.; Morokuma, K.; Rega, N.; Salvador, P.; Dannenberg, J. J.; Malick, D. K.; Rabuck, A. D.; Raghavachari, K.; Foresman, J. B.; Cioslowski, J.; Ortiz, J. V.; Baboul, A. G.; Stefanov, B. B.; Liu, G.; Liashenko, A.; Piskorz, P.; Komaromi, I.; Gomperts, R.; Martin, R. L.; Fox, D. J.; Keith, T.; Al-Laham, M. A.; Peng, C. Y.; Nanayakkara, A.; Challacombe, M.; Gill, P. M. W.; Johnson, B.; Chen, W.; Wong, M. W.; Andres, J. L.; Gonzalez, C.; Head-Gordon, M.; Replogle, E. S.; Pople, J. A. *Gaussian 98*, Revision A.11.4; Gaussian, Inc.: Pittsburgh, PA, 2002.

(17) (a) Becke, A. D. *J. Chem. Phys.* **1993**, *98*, 5648. (b) Lee, C.; Yang, Y.; Parr, R. G. *Phys. Rev. B* **1988**, *37*, 785.

(18) Frisch, M. J.; Pople, J. A.; Binkley, J. S. *J. Chem. Phys.* **1984**, *80*, 3265.

(19) Andrae, D.; Haeussermann, U.; Dolg, M.; Stoll, H.; Preuss, H. *Theor. Chim. Acta* **1990**, *77*, 123.

(20) (a) Prochaska, F. T.; Andrews, L. *J. Chem. Phys.* **1978**, *68*, 5568. (b) Prochaska, F. T.; Andrews, L. *J. Chem. Phys.* **1978**, *68*, 5577. (c) Milligan, D. E.; Jacox, M. E.; McAuley, J. H.; Smith, C. E. *J. Mol. Spectrosc.* **1973**, *45*, 377. (d) Prochaska, F. T.; Andrews, L. *J. Am. Chem. Soc.* **1978**, *100*, 2102. (e) Prochaska, F. T.; Andrews, L. *J. Phys. Chem.* **1978**, *82*, 1731.

(21) Hastie, J. W.; Hauge, R. H.; Margrave, J. L. *J. Chem. Phys.* **1969**, *51*, 2648.

(22) Scott, A. P.; Radom, L. *J. Phys. Chem.* **1996**, *100*, 16502.

(23) Andersson, M. P.; Uvdal, P. *J. Phys. Chem. A* **2005**, *109*, *2937*.

Table 2. Observed and Calculated Fundamental Frequencies of ClC÷TiF$_3$[a]

	ClC÷TiF$_3$		Cl^{13}C÷TiF$_3$	
approximate mode	obsd[b]	calcd (int)	obsd[b]	calcd (int)
ClCTi bend, e		65.3 (0)		64.7 (0)
TiF$_3$ umbrella, a$_1$		178.7 (6)		178.2 (6)
FTiF bend, e		187.1 (5)		185.9 (3)
ClCTi def, e		223.6 (23)		219.1 (24)
(ClC)÷Ti stretch, a$_1$	*c*	400.1 (70)	*c*	399.9 (70)
Ti−F stretch, a$_1$	679.2	699.7 (251)	678.8	699.5 (251)
Ti−F stretch, e	756.6	769.1 (458)	756.6	769.1 (458)
C−Cl Stretch, a$_1$		1135.8 (9)		1098.2 (8)

[a] B3LYP//6-311+G(2d)/SDD level of theory. All frequencies are unscaled and in cm^{-1}, and computed infrared intensities are in km/mol. [b]Argon matrix. [c]Absorption below our spectral limit.

Scheme 1

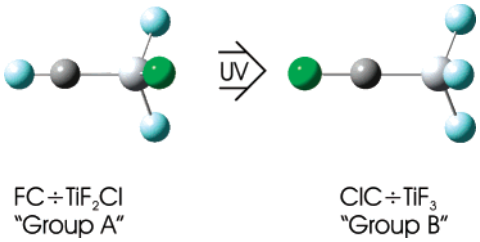

which could be formed on the pathway to the triplet FC÷TiF$_2$-Cl complex assigned to the group A bands. This methylidene species is predicted to be 133 kcal/mol lower in energy than the sum of the reactants. Although it is predicted to have two strong Ti−F stretching modes in this region, at 674.2 and 775.8 cm^{-1}, this complex also has two additional strong modes (C−Cl and C−F stretching) calculated at 835.3 and 1174.3 cm^{-1}. The C−F stretching mode might be hidden behind precursor absorptions, but the C−Cl mode should appear in a clean region of the spectrum. However, no group B absorptions were observed in this region. The second possible product is the triplet ClC÷TiF$_3$ complex, which has C_{3v} symmetry and is 27 kcal/mol lower in energy than the CFCl═TiF$_2$ species. Here the two Ti−F stretching modes are predicted at 699.7 and 769.1 cm^{-1}, reproducing the observed product peaks well for the approximations employed.[13,14,22,23] No other vibrational modes are predicted for this complex above our experimental limit with significant IR intensity (Table 2). Hence, the group B absorptions are assigned to triplet ClC÷TiF$_3$. Scheme 1 summarizes the photochemical rearrangement and provides structural skeletons for the major triplet XC÷MX$_3$ reaction products.

The weak 790.3 cm^{-1} band is most likely due to the TiF$_3$Cl molecule,[24] which is also a straightforward product in this reaction system.[14] Minor weak group C product peaks at 639.3 and 736.4 cm^{-1} did not show a substantial change in intensity during the irradiation and annealing cycles, and a single group D absorption at 744.5 cm^{-1} increased on irradiation with λ > 290 nm and remained constant for the remainder of the experiment. The C absorption at 639.3 cm^{-1} did not show a ^{13}C shift and can be assigned to a Ti−F stretching mode, but the carbon-13 counterpart of the 736.4 cm^{-1} species was not observed. Likewise, the group D absorption at 744.5 cm^{-1} did not shift when ^{13}CF$_3$Cl was used and can also be assigned to a Ti−F stretching mode. Similar to the experiments with Freon-12, CF$_2$Cl$_2$,[14] neither product can be assigned on the basis of the vibrational frequency calculations of possible products. However, we believe that at least one of the minor products is a reactive intermediate formed in the rearrangement of the FC÷TiF$_2$Cl complex to the ClC÷TiF$_3$ species.

(24) Baushlicher, C. W., Jr.; Taylor, P. R.; Komornicki, A. *J. Chem. Phys.* **1990**, *92*, 3982.

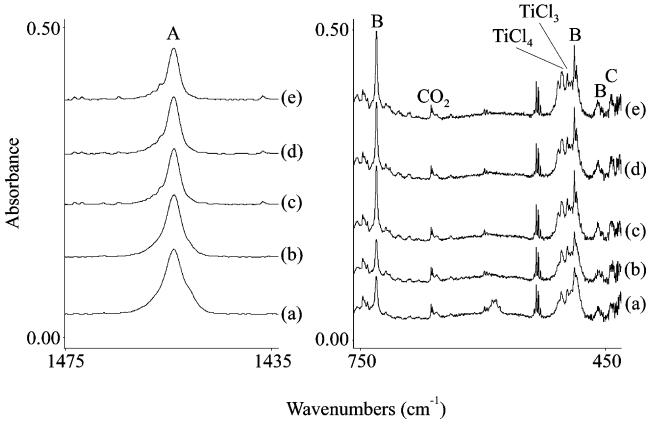

Figure 3. Infrared spectra in the 1475−1430 and 760−430 cm^{-1} regions taken after (a) laser-ablated titanium atoms were reacted with 0.5% CFCl$_3$/Ar during condensation at 8 K for 1 h, and the resulting matrix was subjected to (b) irradiation with light λ > 290 nm, (c) irradiation with λ > 220 nm, (d) annealing to 30 K, and (e) irradiation with λ > 220 nm. Product absorptions labeled A belong to the FC÷TiCl$_3$ complex, B peaks are assigned to the ClC÷TiFCl$_2$ species, and the weak C peak is not identified.

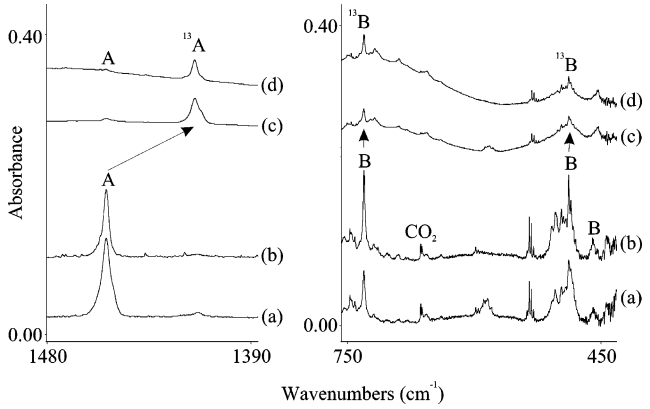

Figure 4. IR spectra in the 1480−1390 and 760−430 cm^{-1} regions of the spectra taken after (a) laser-ablated titanium atoms were reacted with 0.5% CFCl$_3$/Ar, and (b) the matrix sample was irradiated with λ > 220 nm, and after (c) titanium atoms were reacted with 0.1% ^{13}CFCl$_3$/Ar, and (d) the matrix sample was irradiated with λ > 220 nm. Arrows are shown for only A and B product peaks.

Ti + CFCl$_3$. The product absorptions observed after the reactions of titanium atoms with CFCl$_3$ (Freon-11) can be placed into one of four groups on the basis of experimental behavior. One group A absorption observed at 1454.1 cm^{-1} decreased on all photolysis (Figure 3). This absorption showed a 39.2 cm^{-1} carbon-13 isotopic shift (Figure 4) and can be assigned to a strong C−F stretching mode (the C−F stretching mode of the CFCl$_3$ precursor is observed in our matrix environment at 1070 cm^{-1}). Again this diagnostic mode indicates that the group A absorptions belong to the triplet FC÷TiCl$_3$ complex with C_{3v} symmetry, as no other structure is predicted to possess such a high C−F frequency. Our B3LYP calculations predict that two other modes might be observed (Table 3). The second strongest mode (antisymmetric Ti−Cl stretching) for this complex is calculated at 480.1 cm^{-1}. However, it was not observed, as it probably falls underneath the strong TiCl$_4$ and TiCl$_3$ absorptions at 503 and 497 cm^{-1} or the strong B product absorption at 488.2 cm^{-1}. The other mode that might be observed is the (FC)÷Ti stretching mode at 502.6 cm^{-1}. However, this mode is predicted

Table 3. Observed and Calculated Fundamental Frequencies of FC÷TiCl$_3$[a]

	FC÷TiCl$_3$		F^{13}C÷TiCl$_3$	
approximate mode	obsd[b]	calcd (int)	obsd[b]	calcd (int)
FCTi bend, e		59.7 (0)		59.7 (0)
ClTiCl bend, e		111.5 (0)		111.3 (0)
TiCl$_3$ umbrella, a$_1$		118.4 (2)		117.9 (2)
FCTi def, e		228.3 (0)		221.0 (0)
Ti−Cl stretch, a$_1$	*c*	372.5 (9)	*c*	371.7 (8)
Ti−Cl stretch, e	*d*	480.1 (288)	*d*	480.1 (288)
(FC)÷Ti stretch, a$_1$		502.6 (81)		500.9 (80)
C−F stretch, a$_1$	1454.1	1468.1 (493)	1414.9	1427.2 (471)

[a] B3LYP//6-311+G(2d)/SDD level of theory. All frequencies are unscaled and in cm^{-1}, and computed infrared intensities are in km/mol. [b]Argon matrix. [c]Absorption below our spectral limit. [d]Peak hidden behind strong TiCl$_4$, TiCl$_3$, and B product absorptions.

Table 4. Observed and Calculated Fundamental Frequencies of ClC÷TiFCl$_2$[a]

	ClC÷TiFCl$_2$		Cl^{13}C÷TiFCl$_2$	
approximate mode	obsd[b]	calcd (int)	obsd[b]	calcd (int)
ClCTi bend		50.1 (0)		50.0 (0)
ClCTi bend		61.9 (0)		61.5 (0)
ClTiCl bend		113.5 (0)		113.2 (0)
FTiCl bend		146.1 (2)		145.8 (2)
TiFCl$_2$ umbrella		149.3 (2)		148.6 (2)
ClCTi def		218.5 (2)		212.4 (2)
ClCTi def		221.7 (1)		215.3 (1)
(ClC)÷Ti stretch	*c*	365.8 (8)	*c*	365.5 (8)
Ti−Cl stretch	459.3	450.2 (151)		450.2 (151)
Ti−Cl stretch	488.2	485.8 (164)	488.0	485.7 (164)
Ti−F stretch	730.5	747.3 (195)	730.5	747.3 (195)
C−Cl stretch		1130.7 (52)		1093.1 (48)

[a] B3LYP//6-311+G(2d)/SDD level of theory. All frequencies are unscaled and in cm^{-1}, and computed infrared intensities are in km/mol. [b]Argon matrix. [c]Absorption below our spectral limit.

to be 15% as intense as the observed C−F stretching mode and is probably also masked by stronger absorptions near 500 cm^{-1}. Hence, the FC÷TiCl$_3$ complex is characterized by only one, but one very diagnostic, product absorption.

Group B product absorptions at 459.3, 488.2, and 730.5 cm^{-1} did not change in intensity on irradiation with light $\lambda > 290$ nm nor on annealing, but did increase together in intensity after radiation with light $\lambda > 220$ nm (Figure 3). Hence, the three absorptions can be assigned to a single reaction product. The upper absorption at 730.5 cm^{-1} does not show a ^{13}C isotopic shift and can be assigned to a Ti−F stretching mode. The other two group B absorptions are in the region of Ti−Cl stretching modes (Table 4). Therefore, the observed vibrational modes (two Ti−Cl stretching and one Ti−F stretching) clearly indicate the formed product is the triplet ClC÷TiFCl$_2$ complex. Note in Table 4 that the only other vibrational mode predicted to be above our experimental limit is the C−Cl stretching mode, which falls under a strong CFCl$_3$ precursor absorption.

A weak group C absorption at 442.7 cm^{-1} remained constant throughout the experiment. As described previously, this peak cannot be assigned to a specific reaction intermediate.

Ti + CF$_3$Br. Reactions between CF$_3$Br and laser-ablated titanium atoms produced two sets of absorptions, which show noticeable differences throughout the experiment. Analogous group A absorptions at 490.8, 705.3, and 1448.8 cm^{-1} decreased in intensity after exposure to light with $\lambda > 290$ nm, increased slightly after radiation with $\lambda > 220$ nm, increased slightly after annealing to 30 K, and decreased in intensity after a final photolysis with light $\lambda > 220$ nm (Figure S1 in Supporting Information). Note that these are near the group A absorptions for the CF$_3$Cl reaction. The presence of such a high C−F stretching mode confirms that group A absorptions in this experiment arise from the FC÷TiF$_2$Br complex (the antisymmetric C−F stretch of the CF$_3$Br precursor is at 1199 cm^{-1} in our argon matrix). The absorption at 705.3 cm^{-1} matches that predicted for a Ti−F stretching mode in this complex, and the product peak observed at 490.8 cm^{-1} arises from a mode involving the titanium atom stretching against a (CF) subunit. The fourth mode predicted to be above our experimental limit (the second Ti−F stretching mode) is hidden behind our CF$_3$Br precursor absorption (Table S1 in Supporting Information). Hence, the group A absorptions are assigned to the FC÷TiF$_2$Br complex.

Two group B absorptions observed at 645.3 and 737.1 cm^{-1} grew substantially after being exposed to light with $\lambda > 290$ nm, grew slightly after irradiation with $\lambda > 220$ nm light, and remained relatively unchanged throughout the remainder of the experiment (Figure S1). These two absorptions are in the area where we would expect Ti−F stretching modes to appear.[21] Hence, we want to consider two possible products for group B band assignments. The first is the simple CFBr═TiF$_2$ methylidene, which is 15 kcal/mol higher in energy than the identified FC÷TiF$_2$Br complex. The second compound is the triplet BrC÷TiF$_3$ complex, which is 11 kcal/mol lower in energy than the FC÷TiF$_2$Br complex. The group B absorptions grow in during the course of the experiment, while group A bands decreased, indicating that the B product is more stable than the FC÷TiF$_2$Br species and that group B bands may arise from the BrC÷TiF$_3$ complex. Indeed, our vibrational calculations predict that only two modes (the two Ti−F stretching modes) should be in our experimental range with a significant IR intensity (Table S2). Hence, the group B bands are assigned to the triplet BrC÷TiF$_3$ complex.

Zr + CF$_3$Cl. Laser-ablated zirconium atoms reacted with CF$_3$Cl to produce three sets of product absorptions. Group A peaks at 651.3, 658.4, and 1422.4 cm^{-1} increased in intensity on all photolysis and remained constant on annealing (Figure S2). The lower two absorptions did not show a carbon-13 isotopic shift and can be assigned to two Zr−F stretching modes, as they fall in the appropriate region.[25] The third absorption, at 1422.4 cm^{-1}, shifted to 1383.5 cm^{-1} when ^{13}CF$_3$Cl is used in the experiments (Figure 5) and is therefore a strong C−F stretching mode. This frequency is also close to that observed for the FC÷TiF$_2$Cl complex (1452.6 cm^{-1}). The presence of this diagnostic mode, in conjunction with the observation of the two Zr−F stretching modes, and the agreement between the observed peaks and those predicted by our DFT calculations (Table 5) indicate that the group A absorptions can be assigned to the triplet FC÷ZrF$_2$Cl complex.

The two group B absorptions at 584.4 and 645.6 cm^{-1} increased in intensity only after exposure to full-arc radiation ($\lambda > 220$ nm). Again, both absorptions did not show a carbon-13 isotopic shift and can be assigned to Zr−F stretching modes. Considering the same two possible products as we did for titanium, the CFCl═ZrF$_2$ complex is predicted to be 160 kcal/mol lower in energy than the sum of the reactants. Despite the presence of two Zr−F stretching modes for this complex (predicted at 611.7 and 649.6 cm^{-1}), this species is also predicted to have two additional strong modes. However, the C−Cl and C−F stretching modes (predicted at 756.8 and 1185.8 cm^{-1}, respectively) were not observed in the experiment. The second complex that needs to be considered is the triplet ClC÷ZrF$_3$. This species is 42 kcal/mol lower in energy than

(25) Büchler, A.; Berkowitz-Mattuck, J. B.; Dugre, D. H. *J. Chem. Phys.* **1961**, *34*, 2202.

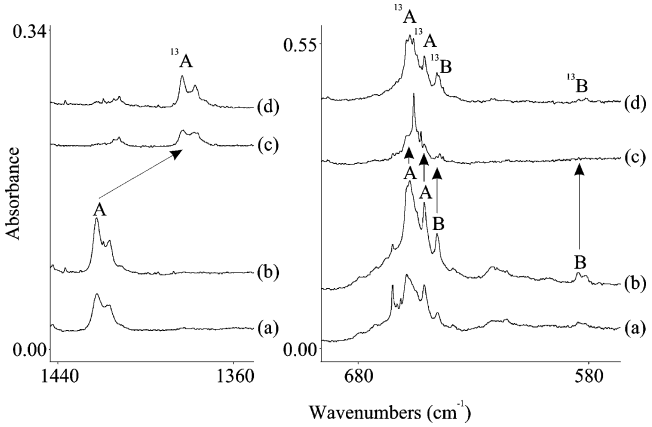

Figure 5. IR spectra in the 1440−1350 and 690−570 cm^{-1} regions of the spectra taken after (a) laser-ablated zirconium atoms were reacted with 0.5% CF_3Cl/Ar, and (b) the matrix sample was irradiated with $\lambda > 220$ nm, and after (c) zirconium atoms were reacted with 0.5% $^{13}CF_3Cl$/Ar, and (d) the matrix sample was irradiated with $\lambda > 220$ nm. Arrows are shown for only A and B product peaks.

Table 5. Observed and Calculated Fundamental Frequencies of $FC{\div}ZrF_2Cl$[a]

	$FC{\div}ZrF_2Cl$		$F^{13}C{\div}ZrF_2Cl$	
approximate mode	obsd[b]	calcd (int)	obsd[b]	calcd (int)
FCZr bend		72.4 (1)		72.4 (1)
FCZr bend		88.9 (2)		88.8 (2)
ClZrF bend		121.9 (3)		121.9 (3)
FZrF bend		135.7 (8)		135.5 (8)
ZrF_2Cl umbrella		151.3 (12)		151.2 (12)
FCZr def		203.5 (7)		197.1 (6)
FCZr def		215.5 (5)		208.5 (5)
Zr−Cl stretch		390.2 (57)		389.5 (54)
(FC)÷Zr stretch	*c*	425.8 (114)	*c*	423.5 (116)
Zr−F stretch	651.3	642.8 (147)	651.3	642.1 (147)
Zr−F stretch	658.4	655.9 (170)	658.4	655.9 (170)
C−F stretch	1422.4	1437.2 (242)	1383.5	1397.2 (234)

[a] B3LYP//6-311+G(2d)/SDD level of theory. All frequencies are unscaled and in cm^{-1}, and computed infrared intensities are in km/mol. [b]Argon matrix. [c]Absorption below our spectral limit.

Table 6. Observed and Calculated Fundamental Frequencies of $ClC{\div}ZrF_3$[a]

	$ClC{\div}ZrF_3$		$Cl^{13}C{\div}ZrF_3$	
approximate mode	obsd[b]	calcd (int)	obsd[b]	calcd (int)
ClCZr bend, e		71.3 (0)		70.9 (0)
ZrF_3 umbrella, a_1		156.0 (13)		155.7 (13)
FZrF bend, e		167.0 (14)		166.6 (12)
ClCZr def, e		194.5 (32)		189.2 (34)
(ClC)÷Zr stretch, a_1	*c*	334.6 (84)	*c*	334.0 (84)
Zr−F stretch, a_1	584.4	635.9 (147)	584.4	635.9 (147)
Zr−F stretch, e	645.6	657.6 (374)	645.6	657.6 (374)
C−Cl stretch, a_1		1095.1 (3)		1058.3 (3)

[a] B3LYP//6-311+G(2d)/SDD level of theory. All frequencies are unscaled and in cm^{-1}, and computed infrared intensities are in km/mol. [b]Argon matrix. [c]Absorption below our spectral limit.

the possible methylidene. Here, the two Zr−F stretching modes are predicted at 635.9 and 657.6 cm^{-1}, accurately reproducing the observed peaks (Table 6). Also, the only other vibration mode predicted above our experimental limit is the C−Cl stretching mode, which is computed to have very little IR activity. Therefore, the two observed group B absorptions are assigned to the $ClC{\div}ZrF_3$ complex with C_{3v} symmetry.

A single broad group C absorption observed at 621.9 cm^{-1} did not change significantly in intensity during the duration of the experiment. This peak did not show a carbon-13 shift, which suggests a Zr−F stretching mode in an unknown intermediate species.

Zr + $CFCl_3$. Freon-11 reacted with laser-ablated zirconium atoms producing two sets of product absorptions distinguishable by product behavior (Figure S3). A single group A absorption at 1433.3 cm^{-1} increased slightly when exposed to UV light with $\lambda > 290$ nm, showed no change when further subjected to light with $\lambda > 220$ nm, increased in intensity when annealed to 30 K, and decreased on a subsequent photolysis with $\lambda > 220$ nm. This group A absorption shifted to 1394.3 cm^{-1} when $^{13}CFCl_3$ was employed, and it can be assigned to a very strong C−F stretching mode (Figure 6). This frequency is 20.8 cm^{-1} lower than that for the analogous $FC{\div}TiCl_3$ species (1454.1 cm^{-1}). The observation of such a strong C−F stretching mode indicates the group A absorption is due to the triplet $FC{\div}ZrCl_3$ complex. The C−F stretch of $FC{\div}ZrCl_3$ is also the only mode predicted by our computations to fall above our experimental limit (Table 7), and its assignment is appropriate.

Two group B absorptions at 655.5 and 417 cm^{-1} increased slightly in intensity on irradiation with $\lambda > 290$ nm, increased significantly with exposure to light with $\lambda > 220$ nm, and did not change on annealing (Figure 6). Both vibrations failed to show ^{13}C isotopic shift and can be assigned to Zr−F and Zr−Cl stretching modes, respectively. These bands are close to analogous stretching modes in the zirconium fluorine and chlorine species in our earlier paper.[14] The observation that the group B absorptions increased in intensity during the course of the experiment at the expense of the group A absorption indicates that the B product is more stable than $FC{\div}ZrCl_3$. The only species that we have computed to be energetically lower in energy than the A product is the triplet $ClC{\div}ZrFCl_2$ (9 kcal/mol lower in energy). Our vibrational computations on this $ClC{\div}ZrFCl_2$ complex find the Zr−F stretching mode at 650.8 cm^{-1} and Zr−Cl stretching mode at 410.7 cm^{-1}, reproducing the observed spectrum well (Table 8). Another possible product, the $CCl_2{=}ZrFCl$ species, is predicted to be 35 kcal/mol higher in energy than the $ClC{\div}ZrFCl_2$ species. Here the possible $CCl_2{=}ZrFCl$ methylidene does have a single Zr−F stretching mode (predicted at 640.1 cm^{-1}), but also has two C−Cl stretches computed at 707.8 and 930.1 cm^{-1}. Although the higher C−Cl mode could be hidden behind a $CFCl_3$ precursor absorption, the lower stretch at 707.8 cm^{-1} should appear in a clean region of the spectrum, but it was not observed. Hence, the group B absorption is assigned to the Zr−F stretching mode of the $ClC{\div}ZrFCl_2$ complex.

Zr + CF_3Br. Laser-ablated zirconium atoms reacted with CF_3Br to produce a single reaction product with infrared absorptions at 650.3, 658.6, and 1422.9 cm^{-1}. These peaks increased slightly in unison upon exposure to light with $\lambda > 290$ nm, increased after full-arc photolysis ($\lambda > 220$ nm), did not change in intensity after annealing to 30 K, and decreased slightly after a subsequent full-arc photolysis (Figure S4). Notice that these three product peaks are all within 1 cm^{-1} of those observed for the $FC{\div}ZrF_2Cl$ complex (refer back to Table 5). The presence of this very strong C−F stretching mode confirms that these group A absorptions belong to the $FC{\div}ZrF_2Br$ complex. The other two observed peaks are in the region of Zr−F stretching modes.[25] Our vibrational frequency calculations predict that only three vibrational modes of the $FC{\div}ZrF_2Br$ complex should be observed in our experiments (Table S3), and the agreement warrants assigning the three observed bands to this complex. The $BrC{\div}ZrF_3$ complex was not observed, but the calculated frequencies are listed in Table S4.

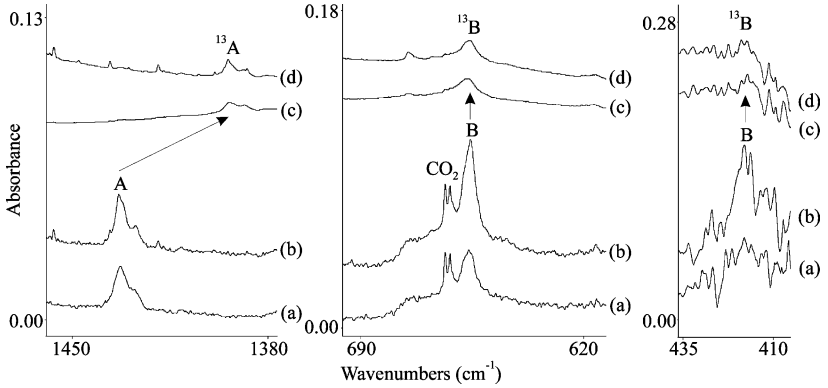

Figure 6. IR spectra in the 1455−1380, 690−615, and 435−410 cm^{-1} regions of the spectra taken after (a) laser-ablated zirconium atoms were reacted with 0.5% $CFCl_3$/Ar, and (b) the matrix sample was irradiated with $\lambda > 220$ nm, and after (c) zirconium atoms were reacted with 0.1% $^{13}CFCl_3$/Ar, and (d) the matrix sample was irradiated with $\lambda > 220$ nm.

Table 7. Observed and Calculated Fundamental Frequencies of FC÷ZrCl$_3$[a]

	FC÷ZrCl$_3$		F^{13}C÷ZrCl$_3$	
approximate mode	obsd[b]	calcd (int)	obsd[b]	calcd (int)
FCZr bend, e		68.0 (0)		67.9 (0)
ClZrCl bend, e		93.9 (2)		93.9 (3)
ZrCl$_3$ umbrella, a$_1$		95.9 (4)		95.7 (4)
FCZr def, e		223.7 (4)		216.2 (4)
Zr−Cl stretch, a$_1$		360.3 (8)		359.8 (7)
Zr−Cl stretch, e		408.0 (238)		408.0 (236)
(FC)÷Zr stretch, a$_1$	*c*	427.4 (84)	*c*	424.8 (83)
C−F stretch, a$_1$	1433.3	1443.5 (334)	1394.3	1403.2 (322)

[a] B3LYP//6-311+G(2d)/SDD level of theory. All frequencies are unscaled and in cm^{-1}, and computed infrared intensities are in km/mol. [b]Argon matrix. [c]Absorption below our spectral limit.

Table 8. Observed and Calculated Fundamental Frequencies of ClC÷ZrFCl$_2$[a]

	ClC÷ZrFCl$_2$		Cl^{13}C÷ZrFCl$_2$	
approximate mode	obsd[b]	calcd (int)	obsd[b]	calcd (int)
ClCZr bend		52.2 (0)		52.2 (0)
ClCZr bend		64.6 (1)		64.4 (1)
ClZrCl bend		96.1 (2)		96.0 (2)
FZrCl bend		122.1 (4)		122.0 (4)
ZrFCl$_2$ umbrella		134.1 (5)		133.5 (5)
ClCZr def		197.1 (6)		190.8 (4)
ClCZr def		197.7 (4)		191.7 (5)
(ClC)÷Zr stretch		327.8 (37)		327.1 (37)
Zr−Cl stretch		386.5 (101)		386.5 (101)
Zr−Cl stretch	417	410.7 (132)	417	410.6 (132)
Zr−F stretch	655.5	650.8 (157)	655.5	650.7 (157)
C−Cl stretch	*c*	1102.5 (17)	*c*	1065.4 (17)

[a] B3LYP//6-311+G(2d)/SDD level of theory. All frequencies are unscaled and in cm^{-1}, and computed infrared intensities are in km/mol. [b]Argon matrix. [c]Peak hidden behind precursor absorption.

Hf + CF$_3$Cl. Laser-ablated hafnium atoms reacted with Freon-13 to yield a single reaction product characterized by three infrared absorptions. Product peaks observed at 641.9, 654.0, and 1433.6 cm^{-1} increased together when exposed to light with $\lambda > 290$ nm and $\lambda > 220$ nm and annealing to 30 K and decreased together during subsequent photolysis with $\lambda > 220$ nm (Figure S5). The lower two absorptions did not show a carbon-13 isotopic shift, indicative of Hf−F stretching modes, but the highest absorption, at 1433.6 cm^{-1}, shifted 39.7 cm^{-1} and can be assigned to a strong C−F stretching mode (Figure 7). These three absorptions match those predicted by our calculations for the triplet FC÷HfF$_2$Cl complex (Table S5). In particular, the C−F stretching mode was not calculated to be this high for any other possible products. In this instance, there is no photoconversion from the observed product to the ClC÷HfF$_3$ complex, but computed frequencies are given in Table S6. This probably has to do with access to an intermediate complex along the transformation pathway, as ClC÷HfF$_3$ is predicted to be 11 kcal/mol lower in energy than FC÷HfF$_2$Cl.

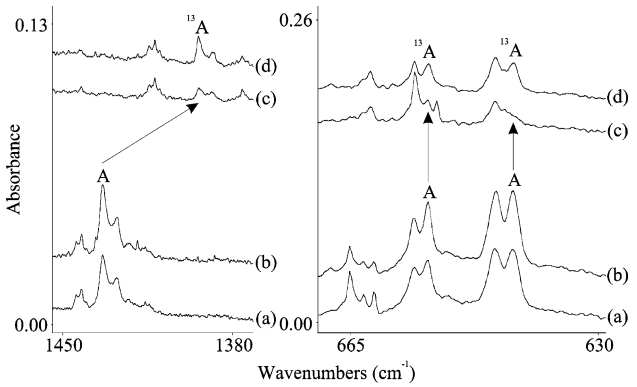

Figure 7. IR spectra in the 1455−1370 and 670−630 cm^{-1} regions of the spectra taken after (a) laser-ablated hafnium atoms were reacted with 0.5% CF_3Cl/Ar, and (b) the matrix sample was irradiated with $\lambda > 220$ nm, and after (c) hafnium atoms were reacted with 0.5% $^{13}CF_3Cl$/Ar, and (d) the matrix sample was irradiated with $\lambda > 220$ nm.

Hf + CFCl$_3$. Freon-11 reacted with hafnium atoms to yield two reaction products, which are distinguishable throughout the experiment. A single group A absorption at 1443.9 cm^{-1} increased slightly after exposure to light with $\lambda > 290$ nm and with $\lambda > 220$ nm, increased significantly after annealing to 30 K, and decreased in intensity after a subsequent photolysis with $\lambda > 220$ nm (Figure S6). This absorption shifted to 1404.1 cm^{-1} when experiments were performed with $^{13}CFCl_3$, indicating a C−F stretching mode. This high C−F stretching mode is the trademark of FC÷MX$_3$ complexes, and hence, we assign the group A absorption to the triplet FC÷HfCl$_3$ species. Additionally, calculations on this complex indicate that the C−F stretching mode (predicted at 1445.9 cm^{-1}) should be the only observed vibrational mode (Table S7).

One group B absorption was also observed in experiments at 649.2 cm^{-1}. This absorption increased slightly in intensity after irradiation with light $\lambda > 290$ nm, increased significantly after exposure to light with $\lambda > 220$ nm, increased slightly after annealing to 30 K, and increased again in intensity after a subsequent photolysis with $\lambda > 220$ nm (Figure S6). This absorption did not show a carbon-13 isotopic shift and can be assigned to a Hf−F stretching mode. This peak grew in intensity on the last full-arc irradiation at the expense of the group A absorption, and it probably belongs to the ClC÷HfFCl$_2$ complex,

Table 9. Geometrical Parameters and Physical Constants of Ground State $X^1C \div MX^2_3$ (M = Ti, Zr, Hf; X = F, Cl)[a]

parameter	$ClC \div TiF_3$	$ClC \div ZrF_3$	$ClC \div HfF_3$	$FC \div TiCl_3$	$FC \div ZrCl_3$	$FC \div HfCl_3$
$r(C-X^1)$	1.634	1.646	1.645	1.266	1.277	1.279
$r(C \div M)$	1.969	2.145	2.141	1.943	2.110	2.114
$r(M-X^2)$	1.765	1.931	1.928	2.198	2.361	2.357
$\angle(CMX^2)$	108.4	109.1	109.4	106.5	107.1	108.2
$\angle(X^2MX^2)$	110.6	109.9	109.5	112.3	111.7	110.7
$q(X^1)$[b]	0.380	0.252	0.320	−0.136	−0.075	−0.082
$q(C)$[b]	−0.674	−0.943	−0.701	−0.022	−0.282	−0.261
$q(M)$[b]	1.235	1.831	1.475	0.757	1.341	1.462
$q(X^2)$[b]	−0.313	−0.380	−0.365	−0.200	−0.328	−0.373
$s(X^1)$[c]	0.221	0.233	0.239	0.102	0.115	0.121
$s(C)$[c]	1.459	1.561	1.599	1.336	1.490	1.544
$s(M)$[c]	0.230	0.157	0.123	0.414	0.278	0.247
$s(X^2)$[c]	0.030	0.016	0.013	0.050	0.039	0.029
μ[d]	3.016	2.257	2.155	2.220	1.643	1.532
ΔE[e]	160	202	207	154	202	204
$\langle s^2 \rangle$[f]	2.010	2.009	2.009	2.008	2.007	2.007

[a] Bond lengths and angles are in Å and deg. All calculations are performed at the B3LYP//6-311+G(2d)/SDD level. Halogens denoted by X are given superscripts depicting their position (see table title). [b]Mulliken atomic charges. [c]Mulliken atomic spin densities. [d]Molecular dipole moment in D. [e]Binding energy in kcal/mol. [f] $\int \Psi^* s^2 \Psi \approx 2.000$ for triplet species; values reported before annihilation of the first spin contaminant.

which is the only species we found to lie lower in energy (by 11 kcal/mol). In addition, the Hf−F stretch is the only mode predicted with observable intensity for the $ClC \div HfFCl_2$ complex (Table S8). All attempts to calculate the $CCl_2{=}HfFCl$ methylidene converged to the lower energy singlet $ClC-HfFCl_2$ complex. Hence, the single group B absorption is assigned to the Hf−F stretching mode of the triplet $ClC \div HfFCl_2$ complex.

Hf + CF_3Br. The reaction between hafnium atoms and CF_3Br created one product with bands observed at 642.0, 652.8, and 1433.8 cm^{-1}. These three infrared absorptions increased slightly together on photolysis with both $\lambda > 290$ nm and $\lambda > 220$ nm, increased significantly after annealing to 30 K, and did not change in intensity upon further photolysis (Figure S7). These three frequencies are again extremely close to those observed for the $FC \div HfF_2Cl$ species (refer to Table S5) and suggests that the observed A bands probably belong to the analogous $FC \div HfF_2Br$ species. The presence of the very strong C−F stretching mode verifies this molecular identity. Finally, the agreement between theory and experiment within the approximations involved[22,23] for the $FC \div HfF_2Br$ complex for three vibrational modes (Table S9) confirms the molecular assignment. Although the $BrC \div HfF_3$ complex was not observed, its calculated frequencies are given in Table S10 for comparison.

Ti, Zr, and Hf + CF_3I. Similar investigations were done for group 4 metals and trifluoromethyl iodide. In the reaction of titanium and CF_3I, two reaction products were formed and characterized (Figure S8). The group A absorptions at 1435.3 and 697.6 cm^{-1} decrease in intensity on UV irradiation, and the group B bands grow in at 677.3 and 756.9 cm^{-1}. On the basis of comparison with theoretical frequency predictions (see Tables S1 and S2), these absorptions are assigned to the $FC \div TiF_2I$ and $IC \div TiF_3$ complexes. Note the strong C−F stretching mode of the $FC \div TiF_2I$ species is 13.5 cm^{-1} redshifted from that of the $FC \div TiF_2Br$ analogue. In zirconium and hafnium reactions, only the $FC \div MF_2I$ complexes are formed (Figure S8; Tables S3 and S5). In like fashion, only the A product was produced in Zr and Hf reactions with CF_3Br.

Reaction Mechanisms. The reaction mechanism has been outlined in our work on Ti and CCl_4,[13,14] and it will be summarized here. This mechanism is based on previous work with halomethanes[9−12] and present calculations of intermediate species, which lead to the lowest energy final product. The group 4 metal atom needs to be excited to initiate the group 4 metal and CX_4 reaction (eq 1) sequence [(S) and (T) note singlet and triplet electronic states and * indicates excess energy from an external source or the reaction exothermicity]. Note the dominance of α-halogen transfer processes in the mecahnism.

$$M^*(T) + CX_4\,(S) \rightarrow [X_3C-MX]^*\,(T) \rightarrow [X_2C-MX_2]^*\,(T) \rightarrow X_2C{=}MX_2\,(S) \rightarrow XC-MX_3{}^*\,(S) \rightarrow XC \div MX_3\,(T) \quad (1)$$

The laser-ablated atoms are excited, and the laser-ablation plume contains the atomic emission lines, which irradiate the sample. In addition ultraviolet irradiation of the deposited samples leads to an overall increase in the product yield, and this is most likely due to electronic excitation of metal atoms trapped near precursor molecules in the cold matrix.

Group Trends and Bonding Considerations. Notice that the C÷M bond length trend with increasing M size in common $XC \div MX_3$ molecules is increasing bond length and spin density on carbon (see tables for data). This arises from decreased C(2p)−M(nd) overlap and less effective π bonding for the heavier metal atoms. Let us consider the $FC \div TiF_3$ and $ClC \div TiCl_3$ molecules, for example, and compare C÷Ti bond lengths and spin densities as a measure of the π-bonding interaction. First, the C÷Ti bond is computed to be shorter in the chlorine species (1.946 Å) than in the fluorine complex (1.967 Å), and the C spin density is less in the chloride species (1.333) than in the fluoride complex (1.467) (in ref 14). This suggests that chlorine substitution on the metal center supports the π-bonding interaction better than fluorine, which arises from more contraction of the metal d orbitals and less effective overlap with carbon by the more electronegative substituent. Second, a similar comparison of $ClC \div TiF_3$ and $FC \div TiCl_3$ (Table 9) reveals a shorter bond for the latter (1.943 Å) than the former (1.969 Å) and further supports this contention. Third, starting with $ClC \div TiCl_3$ the C÷Ti bond length increases stepwise with the number of fluorine substituents at titanium. Further comparison of $FC \div TiFCl_2$ and $FC \div TiF_2Cl$ bond lengths (1.951 and 1.958 Å, respectively) (Table 10) supports this assertion. Thus we expect bromide and iodide to decrease the C÷M bond length and carbon spin density, and this is indeed the case (Tables S11 and S12). The C÷Ti bond length in the $FC \div TiF_2X$ series (X = F, Cl, Br, I) decreases from 1.967 Å to 1.958 Å to 1.955 Å to 1.946 Å as the electronegativity of X decreases. This appears to be due to stronger π bonds with the heavier, less electronegative halide, which has less of a contracting effect on the metal d orbitals. In addition the larger

Table 10. Geometrical Parameters and Physical Constants of Ground State X^{1}C÷MX$_2$^{2}X^3 (M = Ti, Zr, Hf; X = F, Cl)[a]

parameter	FC÷TiF$_2$Cl	ClC÷TiFCl$_2$	FC÷ZrF$_2$Cl	ClC÷ZrFCl$_2$	FC÷HfF$_2$Cl	ClC÷HfFCl$_2$
r(C-X^1)	1.269	1.632	1.280	1.641	1.283	1.642
r(C÷M)	1.958	1.955	2.128	2.125	2.127	2.126
r(M−F)	1.764	1.760	1.929	1.924	1.925	1.921
r(M−Cl)	2.206	2.201	2.371	2.366	2.366	2.363
∠(CMF)	108.0	107.9	108.7	107.9	109.3	108.2
∠(CMCl)	106.1	106.6	108.0	107.8	109.4	109.3
∠(FMCl)	111.5	111.8	110.6	110.7	110.0	110.1
∠(X^{2}MX^2)	111.6	112.0	110.3	111.8	109.1	111.5
q(X^1)[b]	−0.139	0.395	−0.079	0.324	−0.098	0.427
q(C)[b]	−0.156	−0.487	−0.529	−0.675	−0.311	−0.606
q(M)[b]	1.261	1.004	1.833	1.590	1.509	1.287
q(F)[b]	−0.345	−0.343	−0.383	−0.383	−0.343	−0.319
q(Cl)[b]	−0.277	−0.284	−0.460	−0.428	−0.413	−0.395
s(X^1)[c]	0.105	0.214	0.116	0.232	0.122	0.235
s(C)[c]	1.420	1.375	1.556	1.499	1.608	1.550
s(M)[c]	0.357	0.300	0.250	0.186	0.213	0.151
s(F)[c]	0.034	0.029	0.022	0.019	0.017	0.014
s(Cl)[c]	0.050	0.042	0.035	0.032	0.026	0.025
μ[d]	2.252	3.119	1.670	2.435	1.586	2.257
ΔE[e]	148	165	192	211	196	215
$\langle s^2 \rangle$[f]	2.008	2.010	2.007	2.009	2.007	2.009

[a] Bond lengths and angles are in Å and deg. All calculations are performed at the B3LYP//6-311+G(2d)/SDD level. Halogens denoted by X are given superscripts depicting their position (see table title). Halogens denoted F and Cl are not in the X^1 position. [b] Mulliken atomic charges. [c] Mulliken atomic spin densities. [d] Molecular dipole moment in D. [e] Binding energy in kcal/mol. [f] $\int \Psi^* s^2 \Psi \approx 2.000$ for triplet species; values reported before annihilation of the first spin contaminant.

halides accommodate more electron spin density.[26] The computed $\langle s^2 \rangle$ values range from 2.007 to 2.011, indicating that these are well-defined triplet state XC÷MX$_3$ complexes (Tables 9, 10, S11, and S12).

It is intriguing to note that for the hafnium reactions with CF$_3$Cl and CF$_3$Br, as well as for the zirconium reactions with CF$_3$Br, only the FC÷MF$_2$X species (A products) forms (where here X denotes Cl or Br) and there is no photochemical conversion to the XC÷MF$_3$ complex (B products). For all three of these reactions, the latter is predicted to be lower in energy (by 11, 10, and 9 kcal/mol, respectively). For all other reactions studied here, both complexes are observed in the matrix infrared spectra. Clearly, whether or not the rearrangement occurs must have to do with the formation of intermediate species along the conversion pathway. Note that the latter (more energetically favorable group B species) do not form when one of the halogen atoms that needs to be moved is heavier (and transfers slower than the lighter halogens) and when the metal atom is the largest (and there is a further distance for the halogen atom to transfer). However, note that both A and B products form when all three group 4 metal atoms react with CF$_2$Cl$_2$ and CFCl$_3$.[14] Hence, we believe kinetic factors preclude the formation of group B absorptions for heavier metals and halide substituents. The very high C−F stretching frequency in the 1450−1420 cm^{-1} region is diagnostic for the FC÷MX$_3$ complexes.[13,14] In all FC÷MX^1$_2$X^2 cases this frequency decreases from Ti to Zr then increases part way back with Hf. This we believe is due to the relativistic effect in Hf,[27] as in all cases the computed C÷Hf bond length is slightly shorter (or equal to) than the C÷Zr bond length. This will alter the F−C, C÷M mode mixing. We note in the FC÷MF$_2$Cl series the carbon-13 shift in the C−F stretching mode is 2.86%, 2.73%, and 2.77%, respectively, for M = Ti, Zr, and Hf, which shows more (antisymmetric) carbon motion between F and M and is in accord with a higher frequency.

(26) Tables 9, 10, S11, and S12 give the structural parameters calculated for the A and B complexes discussed here.

(27) Pyykko, P. *Chem. Rev.* **1988**, *88*, 563.

Conclusions

Laser-ablated group 4 transition metals reacted with CF$_3$Cl and CFCl$_3$ to form mixtures of triplet FC÷MX$_3$ and ClC÷MX$_3$ complexes. The former complexes are produced during deposition, but are converted to the more stable latter products on UV irradiation. Analogous reactions with CF$_3$Br and CF$_3$I form similar products with Ti, but only the FC÷MX$_3$ analogues with Zr and Hf. These triplet state complexes possess very strong C−X bonds, and the two unpaired electrons on carbon are partially shared with the metal center. The electron-deficient triple bond is characterized in this report on the basis of computed bond lengths (which are near a classical double bond) and the donation of spin density. This work and reaction products with CF$_4$, CF$_2$Cl$_2$, and CCl$_4$ provide a complete data set on the effects of competitive α-halogen transfer. We find that the C÷M bond is longer for the largest number of the most electronegative substituents owing to contraction of the metal d orbitals and decreased π bonding.

Acknowledgment is made to the Donors of the American Chemical Society Petroleum Research Fund for support of this research.

Supporting Information Available: Figures S1 through S8 for infrared spectra and Tables S1 through S12 for calculated frequencies and structural parameters. This material is available free of charge via the Internet at http://pubs.acs.org.

OM0702025